Physics Letters A 375 (2011) 1445–1450

Contents lists available at ScienceDirect

Physics Letters A

www.elsevier.com/locate/pla

Generalization of the simplest autonomous chaotic system

Buncha Munmuangsaen [a], Banlue Srisuchinwong [a,*], J.C. Sprott [b]

[a] Sirindhorn International Institute of Technology (SIIT), Thammasat University, Pathum-Thani 12000, Thailand
[b] Department of Physics, University of Wisconsin, Madison, WI 53706, USA

ARTICLE INFO

Article history:
Received 19 October 2010
Received in revised form 7 February 2011
Accepted 12 February 2011
Available online 16 February 2011
Communicated by C.R. Doering

Keywords:
Chaos
Autonomous
Jerk
2-D map
Lyapunov exponents
Differential equations

ABSTRACT

An extensive numerical search of jerk systems of the form $\dddot{x} + \ddot{x} + x = f(\dot{x})$ revealed many cases with chaotic solutions in addition to the one with $f(\dot{x}) = \pm\dot{x}^2$ that has long been known. Particularly simple is the piecewise-linear case with $f(\dot{x}) = \alpha(1 - \dot{x})$ for $\dot{x} \geqslant 1$ and zero otherwise, which produces chaos even in the limit of $\alpha \to \infty$. The dynamics in this limit can be calculated exactly, leading to a two-dimensional map. Such a nonlinearity suggests an elegant electronic circuit implementation using a single diode.

In 1887, King Oscar II of Sweden announced a prize for anyone who could solve the n-body problem and hence demonstrate stability of the Solar System. The prize was awarded in 1889 to Jules Henri Poincaré for submitting a long paper [1] showing that even the three-body problem has no analytical solution. He also indicated that minute differences in the initial conditions could result in very different solutions after a long time. In the early 1960s, a young meteorologist Edward Lorenz accidentally encountered sensitive dependence on initial conditions while modeling atmospheric convection on a primitive digital computer leading to the discovery of the celebrated three first-order ordinary differential Lorenz equations [2]. In 1976, Rössler [3] found a chaotic system with a single quadratic nonlinearity that is algebraically simpler than the Lorenz system. Many other even simpler chaotic systems were discovered in 1994 by Sprott [4] through an extensive computer search for chaotic systems with five terms and two quadratic nonlinearities or six terms and a single quadratic nonlinearity. One of these cases was conservative and previously known [5,6], but the others were dissipative and apparently previously unknown. In response to this work, Gottlieb [7] pointed out that the conservative case can be written in the explicit third-order scalar form

$$\dddot{x} = -\dot{x}^3 + \ddot{x}(x + \ddot{x})/\dot{x} \tag{1}$$

which he called a 'jerk function' since it involves a third derivative of x. Gottlieb also asked the provocative question, "What is the simplest jerk function that gives chaos?". One response was reported by Linz [8] who showed that the Lorenz and Rössler systems can be written in jerk form but that the resulting equations are relatively complicated. However, he further showed that Sprott's case R [4] can be written as a polynomial with only five terms and a single quadratic nonlinearity in its jerk representation, i.e. $\dddot{x} + \ddot{x} - x\dot{x} + ax + b = 0$, which is more appealing than Eq. (1).

Meanwhile, Sprott also took up Gottlieb's challenge and discovered a particularly simple case

$$\dddot{x} + a\ddot{x} \pm \dot{x}^2 + x = 0 \tag{2}$$

which has only three terms in its jerk representation or five terms in its dynamical system representation with a single quadratic nonlinearity and a single parameter a [9]. Subsequently, Zhang and Heidel [10] rigorously proved that there can be no simpler system with a quadratic nonlinearity. In addition, several examples that have the same algebraic simplicity as Eq. (2) were reported by Malasoma [11].

This raises the question of whether there are other simple chaotic systems of the form

$$\dddot{x} + \ddot{x} + x = f(\dot{x}) \tag{3}$$

where $f(\dot{x})$ is the nonlinear function required for chaos. At least one such a system with a piecewise-nonlinear $f(\dot{x})$ has been previously reported [12]. To find chaotic solutions for each of the specified nonlinear functions $f(\dot{x})$, the systematic numerical search procedure developed in [4,9,13] was employed. In such a procedure, the space of control parameters embedded in the nonlinear

* Corresponding author.
E-mail address: banlue@siit.tu.ac.th (B. Srisuchinwong).

0375-9601/$ – see front matter
doi:10.1016/j.physleta.2011.02.028

Table 1
Some functions $f(\dot{x})$ that produce chaos in Eq. (3).

Case	$f(\dot{x})$	Lyapunov exponents	Dimension
GS1	$\pm 0.1\exp(\mp\dot{x})$	0.1021, 0, −1.1021	2.0926
GS2	$\pm\exp(\mp\dot{x}-2)$	0.1009, 0, −1.1009	2.0917
GS3	$\pm 5.1\cos(\pm\dot{x}+0.1)$	0.0467, 0, −1.0467	2.0446
GS4	$\pm 0.2\tan(\mp\dot{x})$	0.1015, 0, −1.1015	2.0921
GS5	$\pm\operatorname{sgn}(1\mp 4\dot{x})$	0.0530, 0, −1.0530	2.0503
GS6	$\pm\dot{x}^2-0.2\dot{x}^3$	0.0489, 0, −1.0489	2.0466
GS7	$\pm 1/(\dot{x}\pm 2)^2$	0.0945, 0, −1.0945	2.0863
GS8	$-5\dot{x}\pm\lvert 1\pm 5\dot{x}\rvert$	0.1168, 0, −1.1168	2.1046
GS9	$\pm 0.4/\lvert\pm\dot{x}+1\rvert$	0.0670, 0, −1.0670	2.0628
GS10	$\pm 1/\lvert\pm\dot{x}+1\rvert^{0.5}$	0.0420, 0, −1.0420	2.0403
GS11	$\pm 4\sin(\pm\dot{x}+1)-2.2\dot{x}$	0.0659, 0, −1.0659	2.0618
GS12	$\pm\cosh(\dot{x})-0.6\dot{x}$	0.0668, 0, −1.0668	2.0626

function $f(\dot{x})$ and initial conditions have been scanned to find a positive Lyapunov exponent, which is a signature of chaos. By this method, we have found many more such chaotic systems. Some examples of the function $f(\dot{x})$ that produce chaos with simplified parameters are selected and listed in Table 1 along with the numerically calculated Lyapunov exponents [14] in base-e and Kaplan–Yorke dimensions [15]. The Lyapunov exponents were calculated using the method detailed in [16]. The calculation was performed using a fourth-order Runge–Kutta integrator with a step size of 0.01. To enable high precision and to ensure that the chaos is neither a numerical artifact nor a chaotic transient, the process was repeated up to a time of 10^7 with extended 80-bit precision. It was also verified that the result is not sensitive to iteration step size or initial conditions and the solution is noticeably stable. The $\operatorname{sgn}(\dot{x})$ term in case GS5 is approximated by $\tanh(200\dot{x})$ for the purpose of estimating the Lyapunov exponent and confirming the chaos since discontinuities in the flow are known to produce large errors in the calculated Lyapunov exponent [17]. The result is not sensitive to the factor of 200, and any large value would suffice. Note that all cases in Table 1 have mirror image systems characterized by the opposite sign of x and its derivatives but having the same eigenvalues and Lyapunov exponents.

It is interesting to adjust parameters in $f(\dot{x})$ for all cases in Table 1 to maximize the Lyapunov exponent (this will also maximize their Kaplan–Yorke dimensions since the sum of the Lyapunov exponents is always −1). We found that all cases have similar maximum values of their largest Lyapunov exponents of about 0.14 and corresponding Kaplan–Yorke dimensions of about $D_{\mathrm{KY}} = 2.12$. Consequently, an attempt to find an 'optimal' $f(\dot{x})$ that maximizes the Lyapunov exponent (and the corresponding Kaplan–Yorke dimension) by tuning the coefficients of a high-order polynomial for $f(\dot{x})$ was unsuccessful, with many nearly equivalent cases. A typical fourth-order polynomial with a large Lyapunov exponent is $f(\dot{x}) = -0.107 - 0.059\dot{x} - 1.665\dot{x}^2 - 0.707\dot{x}^3 - 0.153\dot{x}^4$, and this function resembles case GS1 in Table 1. Note that all cases have the same constant rate of contraction of −1 (the coefficient of the $\ddot{x}$ term), which corresponds to the sum of Lyapunov exponents. A search of conservative cases with the $\ddot{x}$ term absent did not reveal any with chaotic solutions.

The linear stability of Eq. (3) can be studied from the eigenvalues of the Jacobian matrix

$$J = \begin{bmatrix} 0 & 1 & 0 \\ 0 & 0 & 1 \\ -1 & F' & -1 \end{bmatrix} \tag{4}$$

where F' is the partial derivative of $\dddot{x}$ with respect to $\dot{x}$ evaluated at the equilibrium point $(x, \dot{x}, \ddot{x}) = (f(0), 0, 0)$ by treating x and $\ddot{x}$ as constants. To evaluate the derivative of the signum (sgn) case, we take $|\dot{x}| = \dot{x}\operatorname{sgn}(\dot{x})$, i.e., $\operatorname{sgn}(\dot{x}) = |\dot{x}|/\dot{x}$, and its derivative becomes $\operatorname{sgn}(\dot{x})/\dot{x} - |\dot{x}|/\dot{x}^2$. The characteristic equation of the Jacobian matrix in Eq. (4) is

$$\lambda^3 + \lambda^2 - (F')\lambda + 1 = 0. \tag{5}$$

At the equilibrium point, the system is a spiral node for $F' < -1$ and is a spiral saddle with index 2 for $F' > -1$. At $F' = -1$, the system undergoes a Hopf bifurcation where $\lambda = \pm i$. However, all cases given in Table 1 have one real eigenvalue and a complex-conjugate pair of the form $-a, b \pm ci$ with a, b and c positive. Therefore, all cases in the table are spiral saddles with index 2.

The attractors for the various cases in Table 1 are shown in Fig. 1, all of which resemble the prototype Rössler attractor in a sense that they have a single folded-band structure except case GS4 whose attractor looks like two back-to-back swirled Rössler attractors. Initial conditions are not critical, i.e., no need to be chosen carefully and most initial conditions that lie within basin of attraction can produce chaos, and were taken as (0, 1, 0). Note that Eq. (3) requires two parameters to completely characterize all possible dynamical behaviors. These two parameters are needed to explore and plot the entire parameter space without redundancy. However, the two required parameters can usually be embedded in the general family of functions $f(\dot{x})$. In such a case, Eq. (3) can produce chaos with no additional parameter without loss of generality. It is also possible that chaos can occur when one or even both of these parameters happen to be unity, but that is just coincidental.

The case of $f(\dot{x}) = -A\exp(\dot{x})$, which is case GS1 in Table 1 with $A = 0.1$, is particularly interesting. It has the curious feature of having chaotic solutions in the limit of $A \to 0$ as is evident from its largest Lyapunov exponent and bifurcation diagram (the local maxima of x) shown in Fig. 2, which shows a period-doubling route to chaos. The attractor grows in size as $A \to 0$ since a larger $\dot{x}$ is required to achieve the same nonlinearity as A decreases.

The system in Fig. 2 has a homoclinic orbit for $A = 0.1307$ where the unstable manifold of the equilibrium at (−0.1307, 0, 0) intersects its stable manifold tangentially, resulting in an orbit as shown in Fig. 3. The equilibrium point for this case has eigenvalues $\lambda = -1.5193, 0.2596 \pm 0.7686i$, which satisfies the Shilnikov condition [18] since the absolute value of the real eigenvalue is greater than the absolute value of the real part of the complex eigenvalues, providing a proof of chaos. For this value of A, the largest Lyapunov exponent is near its maximum with a Lyapunov exponent spectrum of (0.1016, 0, −1.1016) and a Kaplan–Yorke dimension of $D_{\mathrm{KY}} = 2.0922$.

More interesting is to perform the linear transformation $x \to x/A$ (so $\dot{x} \to \dot{x}/A$, etc.). Then we have $\dddot{x} + \ddot{x} + x = -A^2\exp(\dot{x}/A)$. This system in the limit of $A \to 0$ can be approximated by the piecewise-linear form $f(\dot{x}) = \alpha(1 - \dot{x})$ for $\dot{x} \geqslant 1$ and zero otherwise, which produces chaos even in the limit of $\alpha \to \infty$. The attractor size is independent of α in this limit, and the system is linear with a reflecting boundary at $\dot{x} = 1$. Its attractor for $\alpha = 10^6$ is shown in Fig. 4. At the reflecting boundary, its trajectory jumps immediately from positive $\ddot{x}$ to negative $\ddot{x}$ and has symmetry about $\ddot{x} = 0$, much like the velocity of a ball bouncing elastically from a hard horizontal surface. A Poincaré section in the x–$\dot{x}$ plane depicted in Fig. 5 shows the points at which the trajectory collides chaotically with the reflecting boundary. Its eigenvalues satisfy $\lambda^3 + \lambda^2 + 1 = 0$ and are given by $\lambda = -1.4655, 0.2327 \pm 0.7925i$. It is apparent that this system has $F' = 0$ (and thus $F' > -1$), and it has eigenvalues of the same form, i.e., $-a, b \pm ci$. Indeed, all cases in Table 1 have these properties. The Lyapunov exponent spectrum for this case is (0.1356, 0, −1.1356), giving an attractor dimension of $D_{\mathrm{KY}} = 2.1194$.

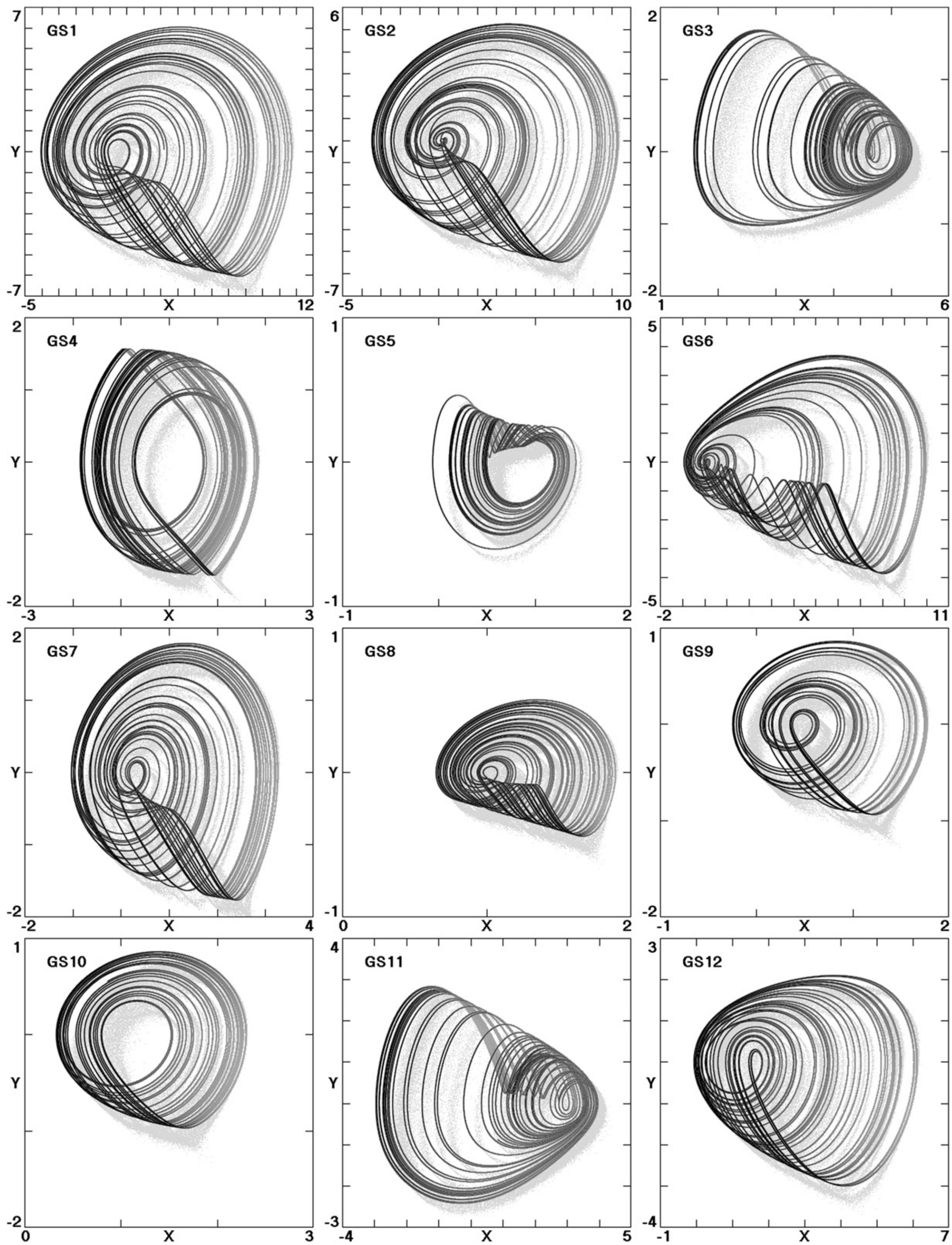

Fig. 1. Attractors of Eq. (3) for each of the nonlinear functions in Table 1.

A great virtue of the piecewise-linear approximation is that the equation can be solved exactly in the two linear regions with a matching condition at the boundary. Thus it is possible to calculate analytically the two-dimensional map that produced the Poincaré section in Fig. 5. The linear ODE that must be solved to get the map of $(x(0), \ddot{x}(0)) \rightarrow (x(T), \ddot{x}(T))$ is $\dddot{x} + \ddot{x} + x = 0$. From the eigenvalues, the solution is of the form $x(t) = A\exp(-at) + \exp(bt)[B\sin\omega t + C\cos\omega t]$ where $a = 1.4655$, $b = 0.2327$, and $\omega = 0.7925$. The values of A, B, and C can be calculated from the specified initial conditions at the boundary. One needs to find the smallest non-zero value of T for which $\dot{x}(T) = 1$, which is the next crossing of the Poincaré plane, by solving for T numerically in the following transcendental equation:

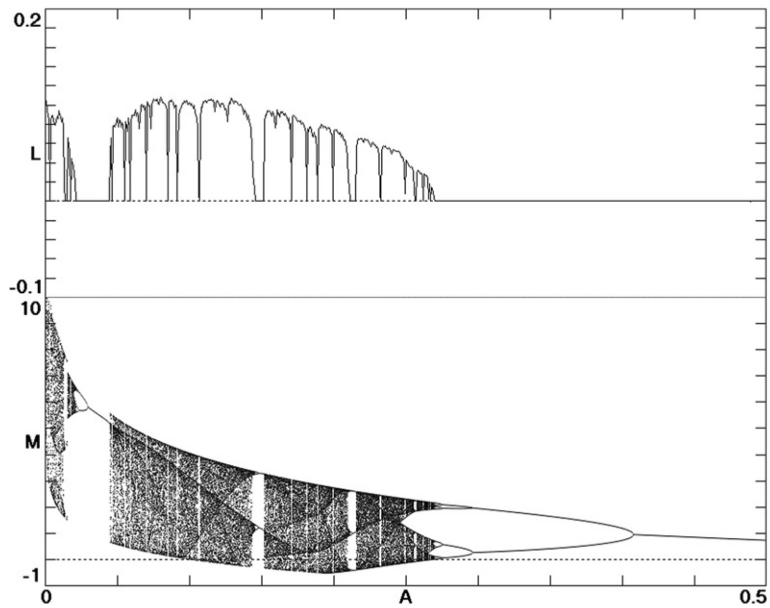

Fig. 2. The largest Lyapunov exponent and bifurcation diagram of Eq. (3) for $f(\dot{x}) = -A\exp(\dot{x})$ with $0 < A < 0.5$.

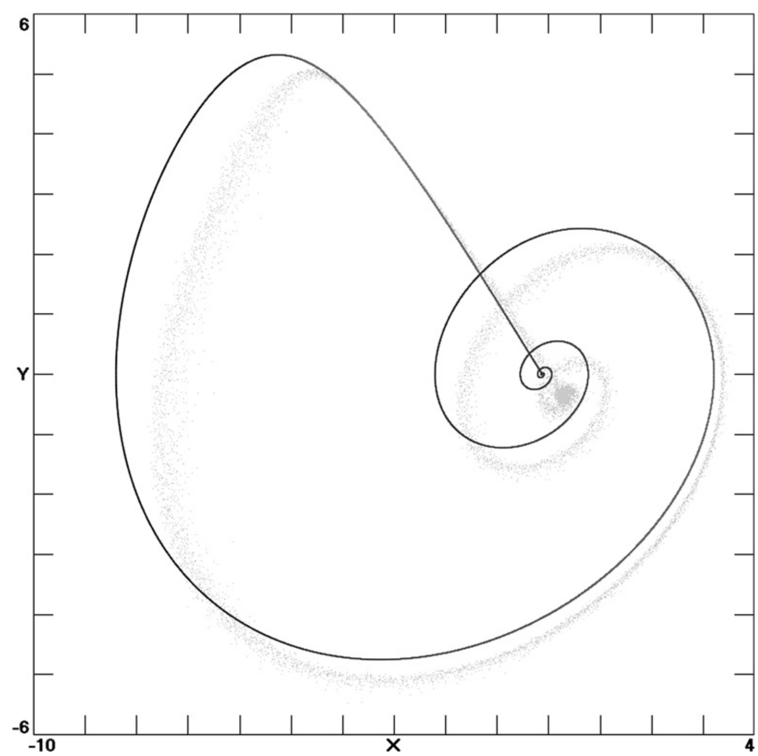

Fig. 3. Homoclinic orbit in Eq. (3) for $f(\dot{x}) = -A\exp(\dot{x})$ with $A = 0.1306$.

$$-aA\exp(-aT) + \exp(bT)[(bB - \omega C)\sin\omega T + (bc + \omega B)\cos\omega T] = 1. \tag{6}$$

Once T is known, it can be substituted into the equations for $x(t)$ and $\ddot{x}(t)$ to get $x(T)$ and $\ddot{x}(T)$. Repeat the process many times to map out the whole Poincaré section. The resulting map looks identical to the Poincaré section in Fig. 5 within round-off errors. Unfortunately, one must solve for T numerically, which means that this is not much of a simplification over solving the ODEs directly, but it is a confirmation that the ODE solution is correct.

The Poincaré section in Fig. 5 appears nearly one-dimensional and suggests that the attractor consists of six nested layers. The fractal structure is not evident because the attractor dimension is only slightly greater than 2.0. However, the fractal structure is exhibited in the return map in Fig. 6, which shows each maximum value of x versus its previous maximum. What looks like two closely spaced lines, upon magnification by a factor of 20, are seen to be six lines. An enlargement by a factor of at least 4×10^3 reveals that each one of which is actually made up of yet more lines in a self-similar fractal structure.

Note that this piecewise-linear function has characteristics resembling a *pn*-junction diode. This fact suggests an elegant elec-

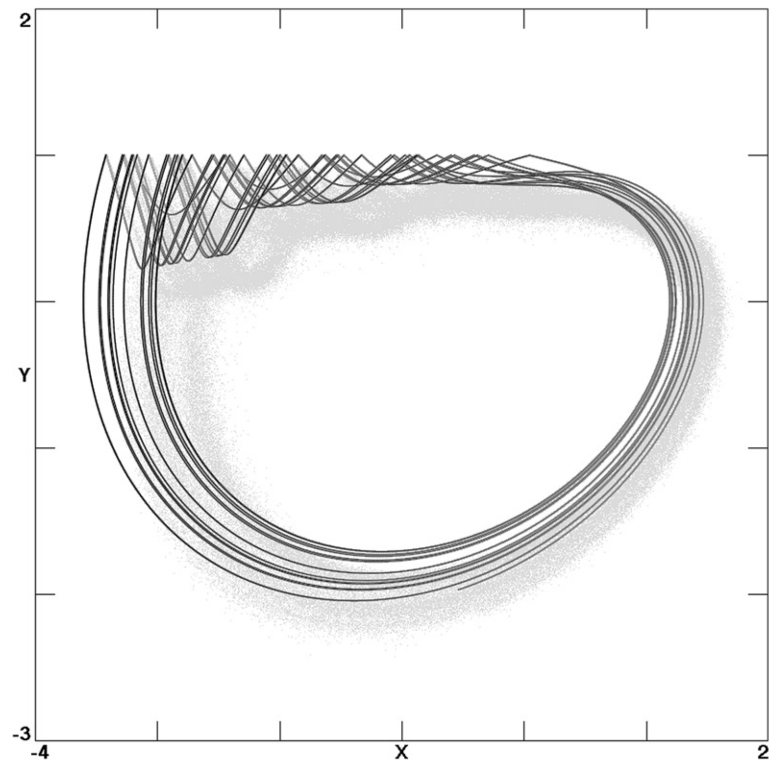

Fig. 4. Attractor for the piecewise-linear system.

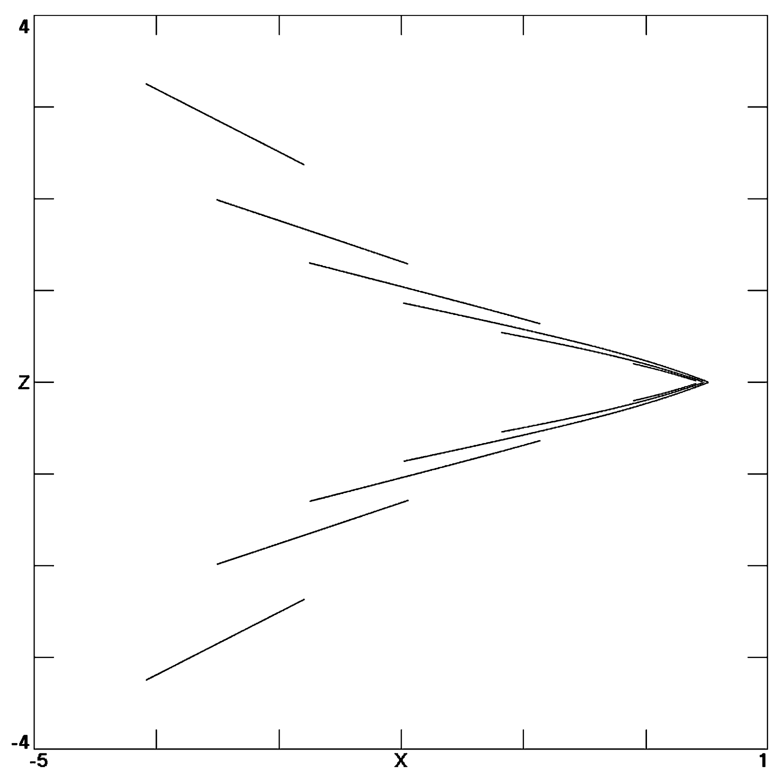

Fig. 5. Poincaré section at $\dot{x} = 0$ for the piecewise-linear system.

tronic circuit implementation using a single diode as the nonlinear element, e.g. a 1N4001 silicon *pn*-junction diode, and it has been investigated and reported in [19].

In conclusion, several simple chaotic systems of the form $\dddot{x} + \ddot{x} + x = f(\dot{x})$ have been studied. They have similar maximum values of their largest Lyapunov exponents and corresponding Kaplan–Yorke dimensions. Furthermore, all cases have $F' > -1$ with spiral saddles of index 2. Particularly simple is the piecewise-linear case with $f(\dot{x}) = \alpha(1 - \dot{x})$ for $\dot{x} \geqslant 1$ and zero otherwise, which produces chaos even in the limit of $\alpha \to \infty$ where the trajectory encounters a reflecting boundary at $\dot{x} = 1$. This system can be calculated exactly, leading to a two-dimensional map identical to the one

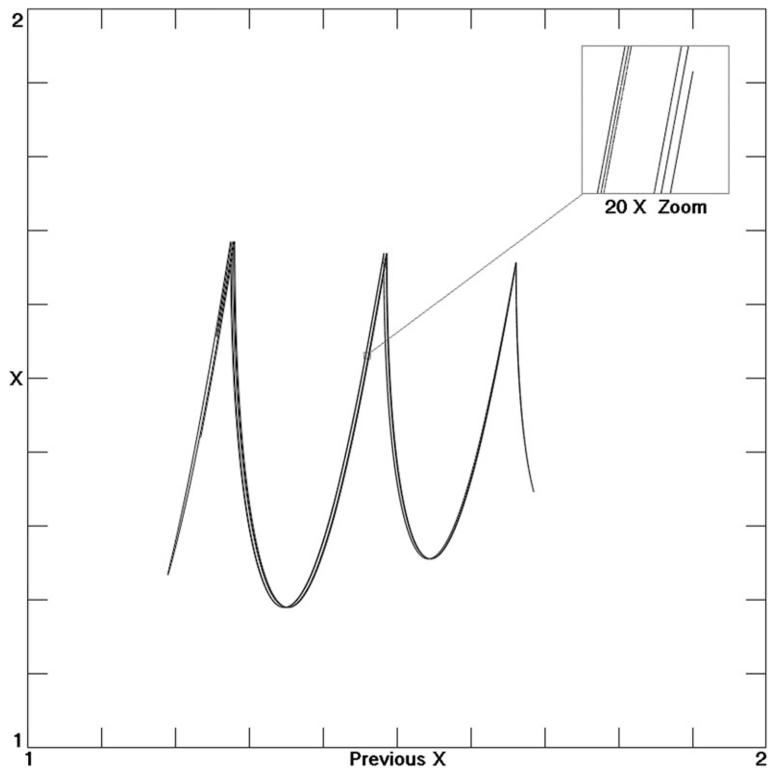

Fig. 6. Return map for the maximum value of x for the piecewise-linear system.

obtained from a numerical solution of the differential equations, and it suggests an elegant electronic circuit implementation using a single diode as the nonlinear element.

Acknowledgements

Buncha Munmuangsaen is grateful to EC-Common Fund of SIIT for the financial support.

References

[1] H. Poincaré, Acta Math. 13 (1890) 1.
[2] E.N. Lorenz, J. Atmospheric Sci. 20 (1963) 130.
[3] O.E. Rössler, Phys. Lett. A 57 (1976) 397.
[4] J.C. Sprott, Phys. Rev. E 50 (1994) R647.
[5] H.A. Posh, W.G. Hoover, F.J. Vesely, Phys. Rev. A 33 (1986) 4253.
[6] W.G. Hoover, Phys. Rev. E 51 (1995) 759.
[7] H.P.W. Gottlieb, Am. J. Phys. 64 (1996) 525.
[8] S.J. Linz, Am. J. Phys. 65 (1997) 523.
[9] J.C. Sprott, Phys. Lett. A 228 (1997) 271.
[10] Z. Fu, J. Heidel, Nonlinearity 10 (1997) 1289.
[11] J.M. Malasoma, Phys. Lett. A 305 (2002) 52.
[12] L.M. Kocic, S. Gegovska-Zajkova, Facta Univ. Ser. Autom. Control Robot. 8 (2009) 35.
[13] J.C. Sprott, Am. J. Phys. 65 (1997) 537.
[14] A. Wolf, J.B. Swift, H.L. Swinney, J.A. Vastano, Physica D 16 (1985) 285.
[15] J.L. Kaplan, J.A. Yorke, in: H.-O. Peitgen, H.-O. Waltber (Eds.), Functional Differential Equations and Approximations of Fixed Points, in: Lecture Notes in Mathematics, vol. 730, Springer, Berlin, 1979, p. 204.
[16] J.C. Sprott, Chaos and Time-Series Analysis, Oxford University Press, Oxford, 2003.
[17] W.J. Grantham, B. Lee, Dynam. Contr. 3 (1993) 159.
[18] L.P. Shilnikov, Soviet Math. Dokl. 6 (1965) 163.
[19] J.C. Sprott, IEEE Transactions on Circuits and Systems (2011), in press.